Digital Resonant Controller based on Modified Tustin Discretization Method

Djordje STOJIC
Nikola Tesla Institute of Electrical Engineering, 11000 Belgrade, Serbia
djordje.stojic@ieent.org

***Abstract*—Resonant controllers are used in power converter voltage and current control due to their simplicity and accuracy. However, digital implementation of resonant controllers introduces problems related to zero and pole mapping from the continuous to the discrete time domain. Namely, some discretization methods introduce significant errors in the digital controller resonant frequency, resulting in the loss of the asymptotic AC reference tracking, especially at high resonant frequencies. The delay compensation typical for resonant controllers can also be compromised. Based on the existing analysis, it can be concluded that the Tustin discretization with frequency prewarping represents a preferable choice from the point of view of the resonant frequency accuracy. However, this discretization method has a shortcoming in applications that require real-time frequency adaptation, since complex trigonometric evaluation is required for each frequency change. In order to overcome this problem, in this paper the modified Tustin discretization method is proposed based on the Taylor series approximation of the frequency prewarping function. By comparing the novel discretization method with commonly used two-integrator-based proportional-resonant (PR) digital controllers, it is shown that the resulting digital controller resonant frequency and time delay compensation errors are significantly reduced for the novel controller.**

***Index Terms*—current control, DC-AC power converters, digital filters, motor drives, three-phase electric power.**

I. INTRODUCTION

Resonant AC current and voltage controllers are widely used in power converter applications, since they enable asymptotic reference tracking. Also, resonant controllers enable effective compensation of the delay introduced by the digital controller sampling and calculation, which significantly improves the control system stability and dynamic performance. Resonant controllers are used in stationary frame based AC control applications, which include: (i) AC motor current controllers [1], (ii) active power filters [2], [3], (iii) active rectifiers [4], (iv) distributed power generation [5], (v) dynamic voltage restorers [6], (vi) fuel cells [7], [8], (vii) photovoltaics [5], and (viii) wind turbines [5]. Resonant controllers are also used in synchronous frame based applications for AC converters with unbalanced loads [9] and unbalanced supply conditions [10].

However, since resonant controllers are in most cases realized in the digital form, the problems of accurate discretization need to be solved in order to preserve the advantageous controller features, namely asymptotic reference tracking and compensation of the time delay. Thus, in order to obtain the discrete equivalent of the continuous-time resonant controller, the following discretization techniques can be applied: (i) backward and forward Euler [11], [12], (ii) Tustin [11], [12], (iii) Tustin with frequency prewarping [13], [14], (iv) zero-order hold [11], [12], and (v) zero-pole mapping [11], [12]. Furthermore, the continuous-time resonator in a double-integrator [15] or any other form can be discretized by means of the delta operator [16]–[18]. Also, special care must be taken if the digital resonant controller is realized by means of fixed-point arithmetic, due to the typical resonant frequency and delay compensation errors caused by the effects of rounding [14], [18].

Since the continuous-time resonant controllers are in many cases realized in the double-integrator form [15] (in order to simplify the frequency adaptation and delay compensation), the related discrete resonant controller is obtained by discretizing the two integrators separately [11], [12], [15].

The resonant continuous-time controller can also be represented in the form of the second-order transfer function, which can be discretized by any of the available techniques and can also include the corresponding delay compensation. Consequently, in [19], a comprehensive analysis of the resonant frequency and delay compensation errors introduced by various discretization techniques is presented, resulting in the following conclusions: (i) the zero-order hold, zero-pole mapping, and Tustin with frequency prewarping techniques are superior to backward and forward Euler, Tustin, and delta operator based discretizations; (ii) however, the former set of techniques suffers from the fact that they require complex calculations (trigonometric, exponential, etc.) when frequency adaptation is required, which is a common requirement in many power converter applications (for example, in AC motor drives).

In order to overcome this problem, a novel resonant controller discretization technique is proposed in this paper, based on the Tustin method with the Taylor series approximation of the frequency prewarping function. It is shown by analytical, simulation, and experimental means that, when compared with other digital resonant controllers that also enable simplified frequency adaptation, the proposed controller operates with minimized resonant frequency and delay compensation errors, especially at high resonant frequencies. The proposed discretization technique is experimentally examined by means of an induction motor (IM) stator current proportional-resonant [20] (PR) digital controller.

This paper consists of four sections. In Section II, the

The work presented in this paper is supported by Ministry of Technology, Education and Science of Republic of Serbia, within the grant TR1652025.

Digital Object Identifier 10.4316/AECE.2016.04013

basic principle of the novel type of resonant controller is outlined, together with the existing types of digital resonant controllers. In Section III, the discretization resonant frequency and time delay compensation errors are examined. In Section IV, experimental tests are presented, based on the IM AC current control implemented by means of the novel type of resonant controller

II. Novel Resonant Controller

A. Different types of resonant controllers in the continuous-time domain

The resonant term is commonly used in conjunction with the proportional term, and together they form the PR controller. However, the PR controller can be implemented with various types of resonant terms [19]: (i) with the cosine Laplace transform based $R_1(s)$ in (1), (ii) with the sine Laplace transform based $R_2(s)$ in (2), and (iii) as the vector proportional-integral (VPI) form of PR controller, consisting of two resonant terms, $R_1(s)$ and $R_3(s)$ in (3). The PR with the cosine resonant term (1) is preferred to PR with the sine term (2), since the zeros introduced in (1) enable more stable controller operation.

$$G_{PR}^{C}(s) = K_P + K_I R_1(s) = K_P + K_I \frac{s}{s^2 + \omega_n^2} \tag{1}$$

$$G_{PR}^{S}(s) = K_P + K_I R_2(s) = K_P + K_I \frac{\omega_n}{s^2 + \omega_n^2} \tag{2}$$

Also, the VPI form (3) of PR controller is preferred in three-phase applications when the plant is in the form $1/(sL_e + R_e)$, since (3) successfully cancels coupling effects between reference frame axes [19].

However, the PR controller can also be successfully used to compensate the delay introduced in the control loop by various effects, for example, by the signal sampling and calculation. Namely, in order to implement the compensation of the time delay $T_d = NT_s$ (where T_s represents the sampling period), the modified type (4) of cosine PR controller (1) can be used.

Furthermore, the VPI type of PR controller (3) can also include the delay compensation by correspondingly modifying each of the resonant terms $R_1(s)$ and $R_3(s)$ to obtain the PR controller (5).

In the following subsection the most commonly used type of PR controller is presented based on two-integrator form.

$$G_{PR}^{VPI}(s) = K_P R_3(s) + K_I R_1(s) = K_P \frac{s^2}{s^2 + \omega_n^2} + K_I \frac{s}{s^2 + \omega_n^2} \tag{3}$$

$$G_{PR}^{dC}(s) = K_P + K_I R_1^d(s) = K_P + K_I \frac{s\cos(\omega_n NT_s) - \omega_n \sin(\omega_n NT_s)}{s^2 + \omega_n^2} \tag{4}$$

$$G_{PR}^{dVPI}(s) = K_P R_3^d(s) + K_I R_1^d(s) = K_P \frac{s^2 \cos(\omega_n NT_s) - s\omega_n \sin(\omega_n NT_s)}{s^2 + \omega_n^2} + K_I \frac{s\cos(\omega_n NT_s) - \omega_n \sin(\omega_n NT_s)}{s^2 + \omega_n^2} \tag{5}$$

B. Implementation of PR controller based on the two-integrator form

The two-integrator form represents a structure commonly used to implement resonant controllers. Namely, it enables simple resonant frequency adaptation, which is crucial in variable-frequency PR applications (for example, AC motor drives). In Fig. 1, two-integrator based forms of $G^{C}_{PR}(s)$ (1) and $G^{VPI}_{PR}(s)$ (3) are presented.

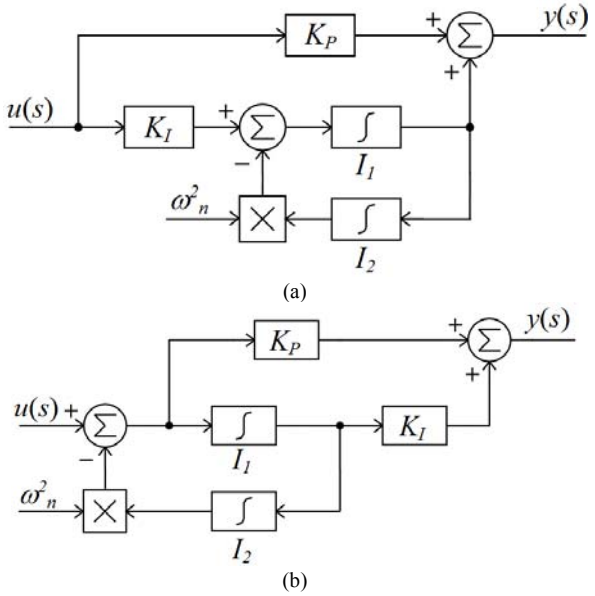

Figure 1. Two-integrator form of (a) $G^{C}_{PR}(s)$ (1) and (b) $G^{VPI}_{PR}(s)$ (3)

Based on Fig. 1, it can be concluded that resonant frequency ω_n adaptation can easily be realized by correspondingly modifying the term ω^2_n.

In the remainder of the paper, the cosine types of PR controllers (1) and (4) are considered for application.

C. Discrete equivalents of continuous-time domain based resonant controllers

The two-integrator based type of PR controller in Fig. 1 is commonly used because it offers (i) easy resonant frequency adaptation and (ii) simple controller discretization. Namely, many authors [19] have proposed the discrete-time PR controller equivalent obtained by individually discretizing each of the integrators I_1 and I_2 in Fig. 1, with the forward and backward Euler [15], [19] discretization methods. However, if forward Euler discretization is used for both integrators I_1 and I_2, an algebraic loop is obtained [11], [12], which is commonly resolved by discretizing the integrator I_1 by means of forward Euler and the integrator I_2 by means of backward Euler, as presented in Fig. 2(a). In Fig. 2(b), the corresponding discrete resonant controller, including compensation of time delay $T_d = NT_s$, is provided.

Nevertheless, in [15] and [19] it is shown that two-integrator based discretization methods introduce significant error in resonant frequency and time delay compensation. Consequently, in [15] the modified two-integrator based discrete PR controller in Fig. 3. is proposed, based on the Taylor series approximation of the term $C_R = \cos(\omega_n T_s) = \omega^2_n - (\omega^4_n T^2_s)/12 + (\omega^6_n T^4_s)/360 - \ldots$. In this way, the resonant controller accuracy is improved, while the simple resonant frequency adaptation is preserved.

In the following subsection, a novel type of digital

resonant controller based on the modified Tustin discretization method is proposed.

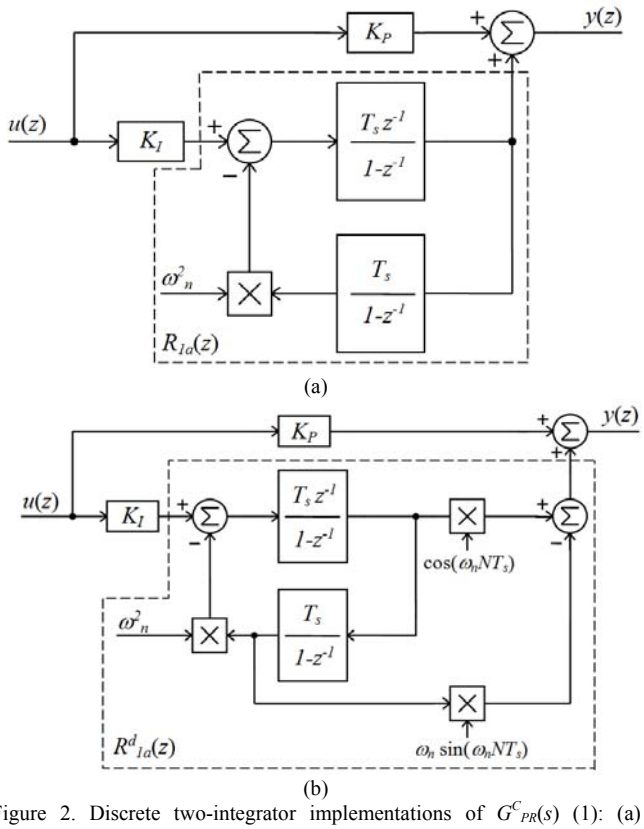

Figure 2. Discrete two-integrator implementations of $G^C_{PR}(s)$ (1): (a) without time delay compensation, and (b) with time delay compensation $T_d = NT_s$

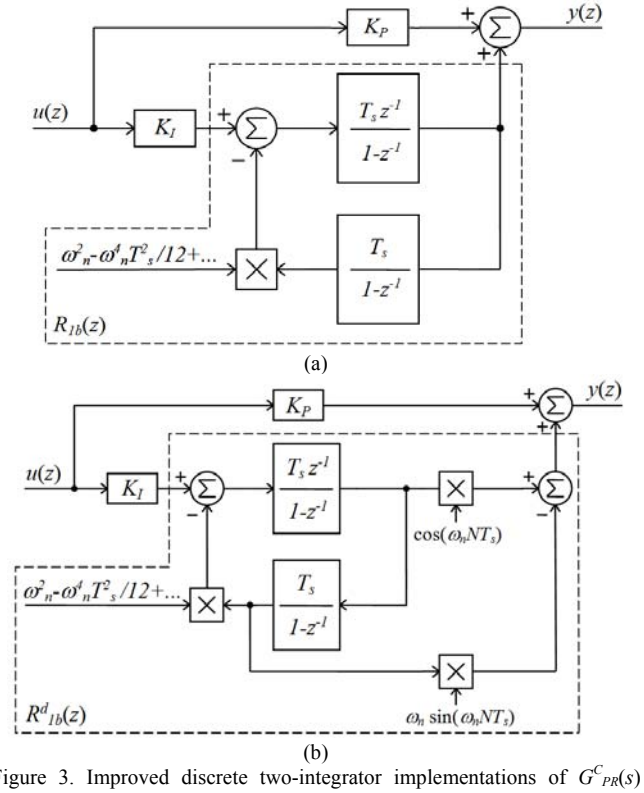

Figure 3. Improved discrete two-integrator implementations of $G^C_{PR}(s)$ based on [15]: (a) without time delay compensation, and (b) with time delay compensation

D. New type of digital resonant controller

The goal of this paper is to propose a new type of digital resonant controller based on the modified Tustin discretization technique with frequency prewarping, which also enables simple resonant frequency adaptation. This is achieved by introducing the Tustin discretization based on the Taylor series approximation of the frequency prewarping function.

Namely, the Tustin discretization with frequency prewarping (6) provides a digital resonant controller that operates with no errors in the resulting resonant frequency value ω_n and delay compensation [19]. This is performed by substituting the Laplace variable s in the continuous-time PR controller transfer function with the term (6).

$$s \leftarrow \frac{\omega_n}{\tan\dfrac{\omega_n T_s}{2}} \frac{z-1}{z+1}, \tag{6}$$

where T_s represents the sampling period.

By observing (6), it can be concluded that complex trigonometric calculations are required for the real-time adaptation of the resonant frequency value ω_n. Consequently, in order to simplify the frequency adaptation, the novel resonant filter discretization technique is proposed based on the Taylor series approximation (7) of the frequency prewarping function (6):

$$f_{prew}(\omega_n) = \frac{\omega_n}{\tan\dfrac{\omega_n T_s}{2}} \approx \frac{2}{T_s} - \frac{T_s\omega_n^2}{6} - \frac{T_s^3\omega_n^4}{360} - \frac{T_s^5\omega_n^6}{15120} - \ldots \tag{7}$$

Consequently, in order to obtain the discrete-time equivalent, the s variable in the continuous-time PR controller transfer function needs to be substituted by (8). However, for systems with smaller sampling frequencies or increased ω_n values, higher elements of the Taylor series (7) should also be included in (8).

$$s \leftarrow \left(\frac{2}{T_s} - \frac{T_s\omega_n^2}{6}\right)\frac{z-1}{z+1} \tag{8}$$

The new discrete equivalent of (1) based on (8) is presented in (9). Also, the novel discrete resonant controller with time delay compensation (4) is presented in (10).

By analyzing (9) and (10), it can be concluded that ω_n resonant frequency adaptation can be performed in a simplified manner, especially when compared to the discrete-time equivalent based on the Tustin discretization with frequency prewarping (6). However, when compared to (6), function (8) introduces errors in the resulting PR controller resonant frequency value and in the time delay compensation. Consequently, in the following section, these errors are compared with those introduced by other types of digital PR controllers that also enable simplified frequency adaptation. In this way, it is shown that the proposed discretization technique enables improved and more accurate PR controller operation.

III. DISCRETIZATION ERRORS

The main goal of the following analysis is to compare three resonant controller discretization methods that are all based on the simplified resonant frequency adaptation. The analysis is performed for two-integrator based PR controllers $R_{1a}(z)$ and $R^d_{1a}(z)$ in Fig. 2, two-integrator based $R_{1b}(z)$ and $R^d_{1b}(z)$ in Fig. 3, and new $R_n(z)$ and $R^d_n(z)$ in (9) and (10) for variable resonant frequency values and variable sampling periods. It is shown that novel discretization introduces significant improvements.

$$G_{PR}^{C}(z) = K_P + K_I R_n(z) = K_P + K_I \frac{a(z^2-1)}{\omega_n^2(z+1)^2 + a^2(z-1)^2}, \text{ with } a = \left(\frac{2}{T_s} - \frac{T_s\omega_n^2}{6}\right) \quad (9)$$

$$G_{PR}^{dC}(z) = K_P + K_I R_n^d(z) = K_P + K_I \frac{a\cos(\omega_n NT_s)(z^2-1) - \omega_n \sin(\omega_n NT_s)(z+1)^2}{\omega_n^2(z+1)^2 + a^2(z-1)^2}, \text{ with } a = \left(\frac{2}{T_s} - \frac{T_s\omega_n^2}{6}\right) \quad (10)$$

A. Resonant frequency discretization errors

For each of the discrete resonator transfer functions $R_{1a}(z)$ in Fig. 2(a), $R_{1b}(z)$ in Fig. 3(a), and $R_n(z)$ in (9), the resulting denominator polynomial has the form $D_i(z) = z^2 - 2z\cos(\omega_r T_s) + 1$, meaning that the digital resonators operate with the resonant frequency ω_r. However, in all three cases the resulting digital resonator resonant frequency ω_r, due to the discretization error, differs from the corresponding continuous time domain PR controller resonant frequency ω_n. Consequently, the goal of the analysis in this subsection is to compare resonant frequency errors introduced by the aforementioned three different types of digital controllers.

In Fig. 4, the resonant frequency discretization error absolute values are presented for the continuous-time PR controller with resonant frequency f_n varying in the range of 0 to 500 Hz, and for the sampling frequency f_s varying in the range of 0 Hz to $0.25f_{nmax}$ (f_{nmax} = 500 Hz). The discretization resonant frequency error eR_{1a} in Fig. 4(a) corresponds to the discrete resonator $R_{1a}(z)$, the error eR_{1b} in Fig. 4(b) corresponds to $R_{1b}(z)$, and the error eR_n in Fig. 4(c) corresponds to $R_n(z)$. By analyzing the results in Fig. 4, it can be concluded that for wide variations of the resonant and sampling frequencies the novel resonator $R_n(z)$ introduces the smallest error (up to two times smaller when compared to $R_{1b}(z)$ and up to 25 times smaller when compared to $R_{1a}(z)$). It should be noted that in all cases the discretization error increases by increasing the resonant frequency f_n and by decreasing the sampling frequency f_s.

B. Time delay compensation errors

The discrete resonators $R^d_{1a}(z)$ in Fig. 2(b), $R^d_{1b}(z)$ in Fig. 3(b), and $R^d_n(z)$ in (10) are used to compensate the time

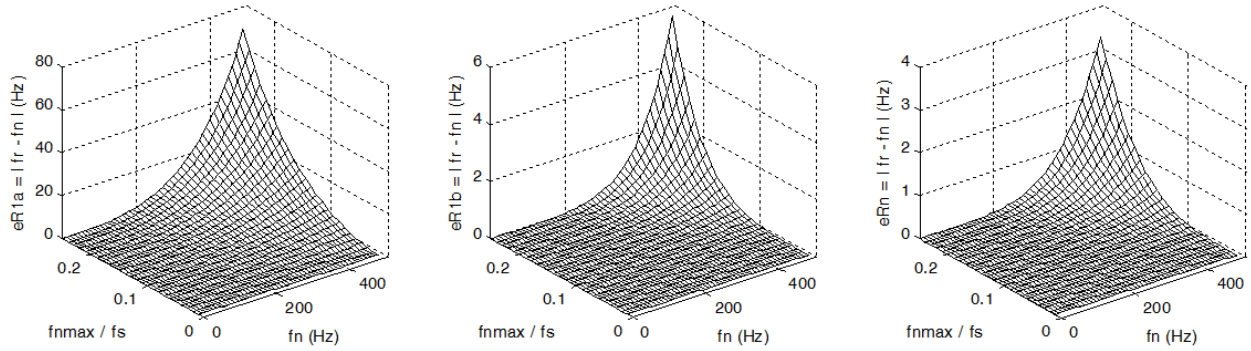

(a) (b) (c)

Figure 4. Resonant frequency discretization error absolute values for (a) $R_{1a}(z)$, (b) $R_{1b}(z)$, and (c) $R_n(z)$

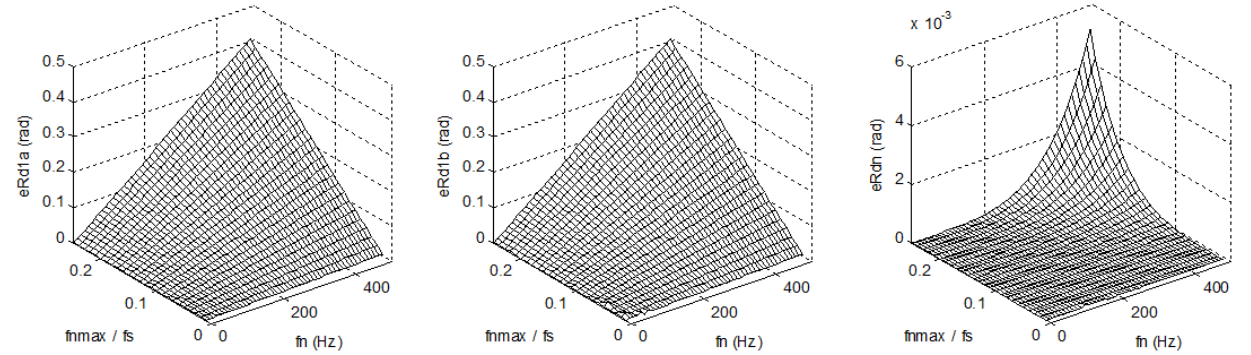

(a) (b) (c)

Figure 5. Delay angle compensation error absolute values for (a) $R^d_{1a}(z)$, (b) $R^d_{1b}(z)$, and (c) $R^d_n(z)$

delay. In this subsection, in order to simplify the error analysis, the compensation of a constant angle value $\varphi = \pi/4$ rad is performed (i.e., in $R^d_{1a}(z)$, $R^d_{1b}(z)$, and $R^d_n(z)$, the term $N\omega_n T_s$ is substituted with φ).

By analyzing the delay angle φ compensation errors in Fig. 5, a similar conclusion to that in [19] can be drawn: that the resonant controller discretization based on the modified Tustin with frequency prewarping $R^d_n(z)$ (10) enables superior delay angle compensation when compared to $R^d_{1a}(z)$ and $R^d_{1b}(z)$. Namely, the delay angle compensation is up to 80 times smaller for $R^d_n(z)$ than for $R^d_{1a}(z)$ and $R^d_{1b}(z)$.

Consequently, based on the error analysis given in Section III, it can be concluded that the novel discrete resonant terms (9) and (10) enable improved operation due to the reduced resonant frequency and delay angle compensation errors.

In the following section, the performance of novel digital resonant action is examined by means of experimental tests.

IV. Experimental Tests

In Section IV, the dynamic performance of the new digital PR controller (10) is examined by means of the IM

stationary frame stator current control. Namely, based on the analysis in Section III, the novel digital resonant controller (10) operates with a reduced resonant frequency discretization error, which is verified by examining the stator current response harmonic contents. Also, the novel controller (10) enables accurate time delay compensation, which is verified by examining the IM stator current responses. Compensation of the time delay equal to $T_d = 2T_s$ is employed, which is typical for the current sampling and pulse-width modulation (PWM) updating techniques used in this paper.

The experimental setup, presented in Fig. 6, consists of the PWM controlled three-phase voltage-source inverter operating with a switching and sampling frequency of 5 kHz, a 1 kW induction motor, and a floating point digital signal processor based control card.

A. Verification of the accuracy of the resonant frequency

The accuracy of the resonant frequency is examined by means of the fast Fourier transform (FFT) analysis of the stator current error signal for the PR controller (10). Namely, if in the error signal no trace of the fundamental frequency component is found, it would suggest that the digital PR controller operates with an accurate discrete resonant frequency, resulting in asymptotic reference tracking. The experiments are performed for two resonant frequencies: $\omega_n = 300$ r/sec and $\omega_n = 1000$ r/sec.

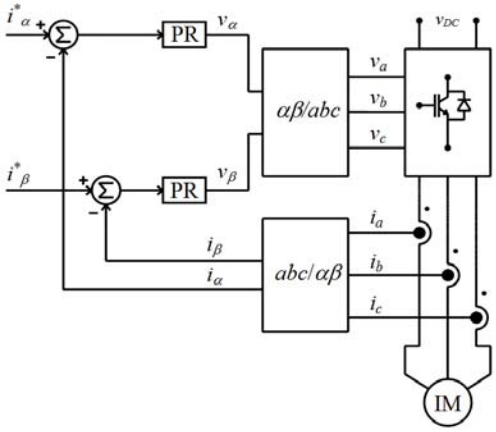

Figure 6. Proportional-resonant stationary frame based induction motor stator current controller

By analyzing the stator current responses in Fig. 7, it can be concluded that no dominant component is found at frequencies equal to $\omega_n = 300$ r/sec in Fig. 7(b) and $\omega_n = 1000$ r/sec in Fig. 7(d), meaning that the PR controller employed operates with zero steady-state error and that the

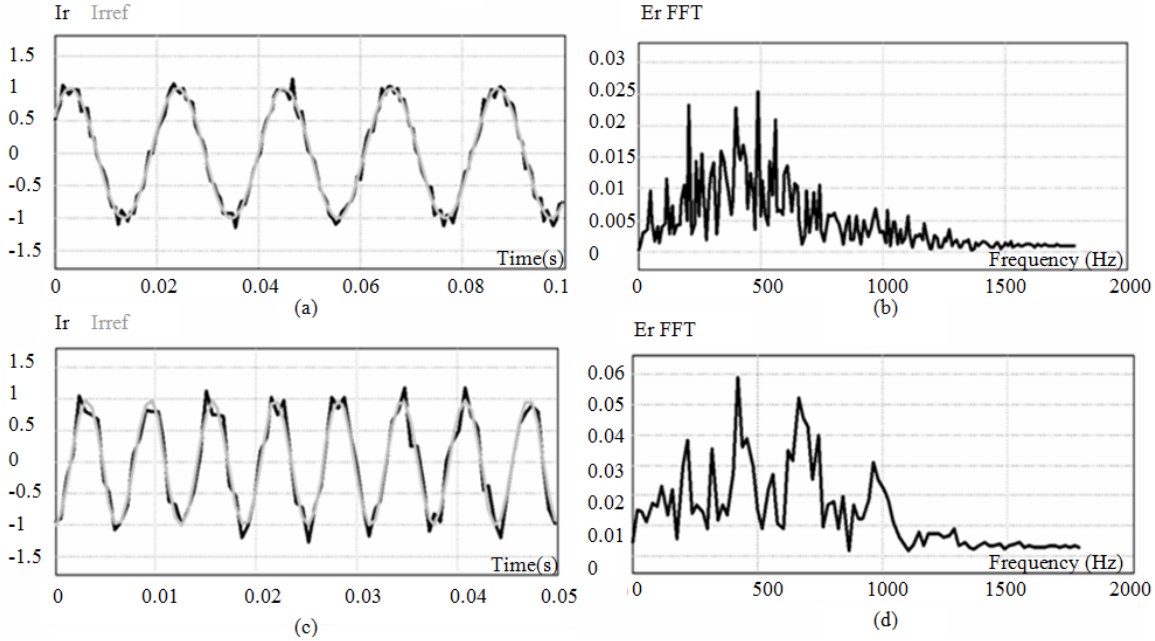

Figure 7. Stator current responses (a) I_r and I^*_r for $\omega_n = 300$ r/sec, (b) FFT of the error signal $e_r = I^*_r - I_r$ for $\omega_n = 300$ r/sec, (c) I_r and I^*_r for $\omega_n = 1000$ r/sec, (d) FFT of the error signal $e_r = I^*_r - I_r$ for $\omega_n = 1000$ r/sec

proposed resonant controller discretization technique results in an accurate resonant frequency value.

B. Delay compensation

In this subsection, the PR controller delay compensation is investigated for the time delay $T_d = 2T_s = 2 / f_s$, where the sampling frequency is equal to $f_s = 5$ kHz. In Fig. 8, the stator current step responses are presented. By analyzing the stator current I_d component responses for $\omega_n = 300$ r/sec without the delay compensation in Fig. 8(a) and with the delay compensation in Fig. 8(b), it can be concluded that the introduction of the delay compensation reduces the stator current overshoot from 50 to 25%. By analyzing the step responses for $\omega_n = 1000$ r/sec without the delay compensation in Fig. 8(c) and with the delay compensation in Fig. 8(d), a similar conclusion can be drawn: that the inclusion of delay compensation improves the stator current response and reduces its overshoot from 40 to 10%.

V. CONCLUSION

In this paper, a novel resonant controller discretization technique based on modified Tustin discretization with a frequency prewarping function is proposed. The main goal of the paper is to propose the resonant controller discretization that operates with minimal resonant frequency and delay compensation errors and that also enables simple frequency adaptation, which is crucial in various power

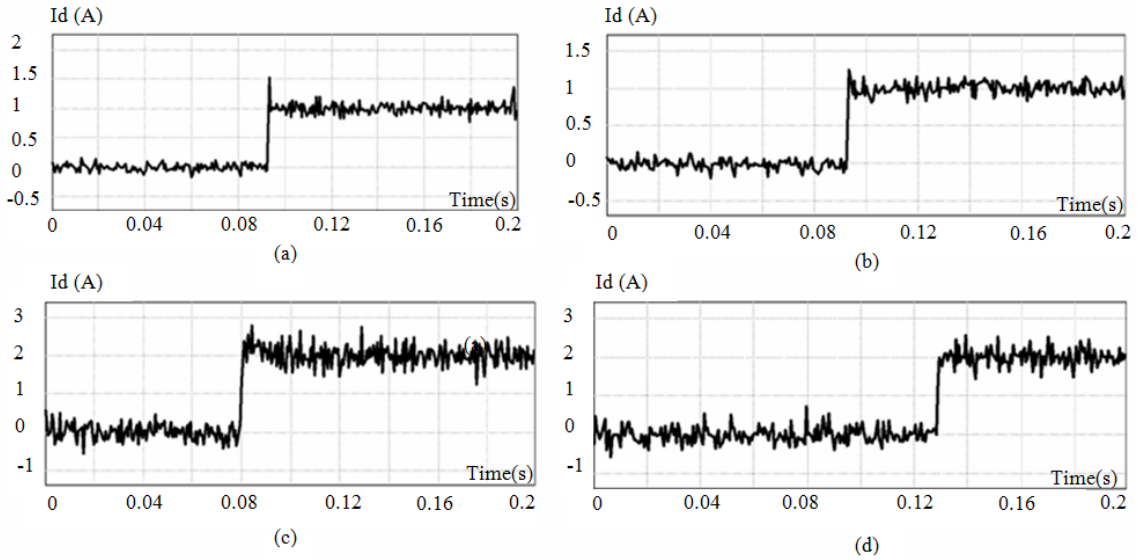

Figure 8. Stator current step responses for: (a) ω_n = 300 r/sec without the delay compensation, (b) ω_n = 300 r/sec with the delay compensation, (c) ω_n = 1000 r/sec without the delay compensation, and (d) ω_n = 1000 r/sec with the delay compensation

converter applications. Consequently, the discretization is proposed based on the Tustin method with Taylor series approximation of the prewarping function. Experimental tests show that the proposed PR controller operates with accurate resonant frequency values and delay compensation, which improves the overall dynamic performance of the IM stator current controller.

REFERENCES

[1] D. G. Holmes, B. P. McGrath, and S. G. Parker, "Current regulation strategies for vector-controlled induction motor drives," Industrial Electronics, IEEE Transactions on, vol. 59, pp. 3680–3689, 2012. doi: 10.1109/TIE.2011.2165455

[2] A. G. Yepes, F. D. Freijedo, J. Doval-Gandoy, O. Lopez, J. Malvar, and P. Fernandez-Comesa, "On the discrete-time implementation of resonant controllers for active power filters," in Industrial Electronics, 2009 (IECON'09). 35th Annual Conference of IEEE, 2009, pp. 3686–3691. doi: 10.1109/IECON.2009.5415136

[3] L. Asiminoaei, F. Blaabjerg, S. Hansen, and P. Thogersen, "Adaptive compensation of reactive power with shunt active power filters," Industry Applications, IEEE Transactions on, vol. 44, pp. 867–877, 2008. doi: 10.1109/TIA.2008.921366

[4] A. D. Aquila, M. Liserre, V. G. Monopoli, and P. Rotondo, "Overview of PI-based solutions for the control of DC buses of a single-phase H-bridge multilevel active rectifier," Industry Applications, IEEE Transactions on, vol. 44, pp. 857–866, 2008. doi: 10.1109/TIA.2008.921405

[5] A. Timbus, M. Liserre, R. Teodorescu, P. Rodriguez, and F. Blaabjerg, "Evaluation of current controllers for distributed power generation systems," Power Electronics, IEEE Transactions on, vol. 24, pp. 654–664, 2009. doi: 10.1109/TPEL.2009.2012527

[6] Y. W. Li, F. Blaabjerg, D. M. Vilathgamuwa, and P. C. Loh, "Design and comparison of high performance stationary-frame controllers for DVR implementation," Power Electronics, IEEE Transactions on, vol. 22, pp. 602–612, 2007. doi: 10.1109/APEC.2006.1620647

[7] S.-Y. Park, C.-L. Chen, and J.-S. J. Lai, "A wide-range active and reactive power flow controller for a solid oxide fuel cell power conditioning system," Power Electronics, IEEE Transactions on, vol. 23, pp. 2703–2709, 2008. doi: 10.1109/TPEL.2008.2003959

[8] S.-Y. Park, C.-L. Chen, J.-S. Lai, and S.-R. Moon, "Admittance compensation in current loop control for a grid-tie LCL fuel cell inverter," Power Electronics, IEEE Transactions on, vol. 23, pp. 1716–1723, 2008. doi: 10.1109/TPEL.2008.924828

[9] R. Cárdenas, C. Juri, R. Peña, P. Wheeler, and J. Clare, "The application of resonant controllers to four-leg matrix converters feeding unbalanced or nonlinear loads," Power Electronics, IEEE Transactions on, vol. 27, pp. 1120–1129, 2012. doi: 10.1109/TPEL.2011.2128889

[10] G. Bergna, J. A. Suul, E. Berne, P. Egrot, P. Lefranc, J.-C. Vannier, et al., "Mitigating DC-side power oscillations and negative sequence load currents in modular multilevel converters under unbalanced faults-first approach using resonant PI," in 38th Annual Conference on IEEE Industrial Electronics Society (IECON 2012), 2012, pp. 537–542. doi: 10.1109/IECON.2012.6388769

[11] F. Rodriguez, E. Bueno, M. Aredes, L. Rolim, F. A. Neves, and M. C. Cavalcanti, "Discrete-time implementation of second order generalized integrators for grid converters," in Industrial Electronics, 2008 (IECON 2008). 34th Annual Conference of IEEE, 2008, pp. 176–181. doi: 10.1109/IECON.2008.4757948

[12] R. Teodorescu, F. Blaabjerg, U. Borup, and M. Liserre, "A new control structure for grid-connected LCL PV inverters with zero steady-state error and selective harmonic compensation," in Applied Power Electronics Conference and Exposition, 2004 (APEC '04). Nineteenth Annual IEEE, 2004, pp. 580–586. doi: 10.1109/APEC.2004.1295865

[13] D. Luczak, "Tunable digital filter structures for resonant frequency effect reduction in direct drive," in Communication Systems, Networks & Digital Signal Processing (CSNDSP), 2012, 8th International Symposium on, 2012, pp. 1–6. doi: 10.1109/CSNDSP.2012.6292777

[14] S. A. Khajehoddin, M. Karimi-Ghartemani, P. K. Jain, and A. Bakhshai, "A resonant controller with high structural robustness for fixed-point digital implementations," Power Electronics, IEEE Transactions on, vol. 27, pp. 3352–3362, 2012. doi: 10.1109/TPEL.2011.2181422

[15] A. G. Yepes, F. D. Freijedo, O. López, and J. Doval-Gandoy, "High-performance digital resonant controllers implemented with two integrators," Power Electronics, IEEE Transactions on, vol. 26, pp. 563–576, 2011. doi: 10.1109/TPEL.2012.2191981

[16] M. J. Newman and D. G. Holmes, "Delta operator digital filters for high performance inverter applications," Power Electronics, IEEE Transactions on, vol. 18, pp. 447–454, 2003. doi: 10.1109/PSEC.2002.1022373

[17] R. Teodorescu, F. Blaabjerg, M. Liserre, and P. C. Loh, "Proportional-resonant controllers and filters for grid-connected voltage-source converters," in Electric Power Applications, IEE Proceedings, 2006, pp. 750–762. doi : 10.1049/ip-epa:20060008

[18] L. Harnefors, "Implementation of resonant controllers and filters in fixed-point arithmetic," Industrial Electronics, IEEE Transactions on, vol. 56, pp. 1273–1281, 2009. doi: 10.1109/TIE.2008.2008341

[19] A. G. Yepes, F. D. Freijedo, J. Doval-Gandoy, O. Lopez, J. Malvar, and P. Fernandez-Comesa, "Effects of discretization methods on the performance of resonant controllers," Power Electronics, IEEE Transactions on, vol. 25, pp. 1692–1712, 2010. doi: 10.1109/TPEL.2010.2041256

[20] C. P. Ion and C. Marinescu, "Autonomous Three-Phase Induction Generator Supplying Unbalanced Loads," Advances in Electrical and Computer Engineering, vol. 13, pp. 85-90, 2013. doi: 10.4316/AECE.2013.0201